AGU PUBLICATIONS

Journal of Geophysical Research: Oceans

Supporting Information for

Basal melting and oceanic observations beneath Fimbulisen, East Antarctica

Katrin Lindbäck[1,2], Elin Darelius[3,4], Geir Moholdt[1], Irena Vaňková[5], Tore Hattermann[1], Julius Lauber[1,3], and Laura de Steur[1]

[1] Norwegian Polar Institute, Tromsø, Norway.

[2] Mid Sweden University, Östersund, Sweden.

[3] Geophysical Institute, University of Bergen, Bergen, Norway.

[4] Bjerknes Centre for Climate Research, Bergen, Norway.

[5] Los Alamos National Laboratory, Los Alamos, NM, USA.

Contents of this file

Introduction

This document includes an extended description of methods, four additional figures, one table supporting the Data and Methods and Results sections of the paper, and references.

Text S1. Data and Methods

Uncertainty in basal melt rate parameterization

To determine the uncertainty in parameterized melt s_m we used standard analytical error propagation methods (Taylor, 1996) with specified uncertainties for each parameter:

$$s_m = \sqrt{\frac{\partial h}{\partial C_0}^2 s_{C0}^2 + \frac{\partial h}{\partial U}^2 s_U^2 + \frac{\partial h}{\partial T}^2 s_T^2} \qquad (1)$$

where s_{C0} represents the standard error of the constant C_0, propagating the standard deviation of m, U and T in Eq. (1). s_U represents the standard deviation of the current velocities U and s_T represents the standard deviation of the ocean temperatures T. By assessing these potential sources of errors, the maximum vertical root-mean-squared uncertainty was calculated to be ±0.6 m yr^{-1}.

Since we lack temperature data from the upper sensor during the ApRES period, we have ignored the effect of temperature variability on melt rates. We can estimate its contribution to the mean melt rate and the variability in melt by considering $U = U_{mean} + U'$, and $T^*=T^*_{mean}+T^{*\prime}$ where "mean" denotes deployment mean. We then get:

$$UT^* = U_{mean}T^*_{mean} + U_{mean}T^{*\prime} + U'T^*_{mean} + U'T^{*\prime} \qquad (2)$$

and

$$(UT^*)_{mean} = (U_{mean}T^*_{mean}) + (U'T^{*\prime})_{mean} \qquad (3)$$

(since $U'_{mean}=T^{*\prime}_{mean} = 0$ per definition). Using the data from the period with both temperature and velocity measurements from the upper sensor, we get that the contribution from $(U'\,T')_{mean}$ to $(U\,T^*)_{mean}$ (and hence to the mean melt rate) is about 1 % and the term can safely be neglected when estimating C_0. We lack information about $T^{*\prime}$ for the ApRES-period and we are thus forced to simplify Eq. (4):

$$U\,T^*{}_{resolved} \approx U_{mean}\,T^*_{mean} + U'\,T^*{}_{mean} \qquad (4)$$

The correlation between $U\,T^*_{resolved}$ and the full $U\,T^*$ is high (for the period 2009 to 2016) as $T^{*\prime}$ mainly modifies the size of the peaks (Fig. S4). The standard deviation of the residuals, $std(U\,T^* - U\,T^*_{resolved})$ is smaller than the standard deviation of the full $U\,T^*$ by a factor of about 1/3, whereas the standard deviation of $U\,T^*_{resolved}$ roughly equals that of $U\,T^*$.

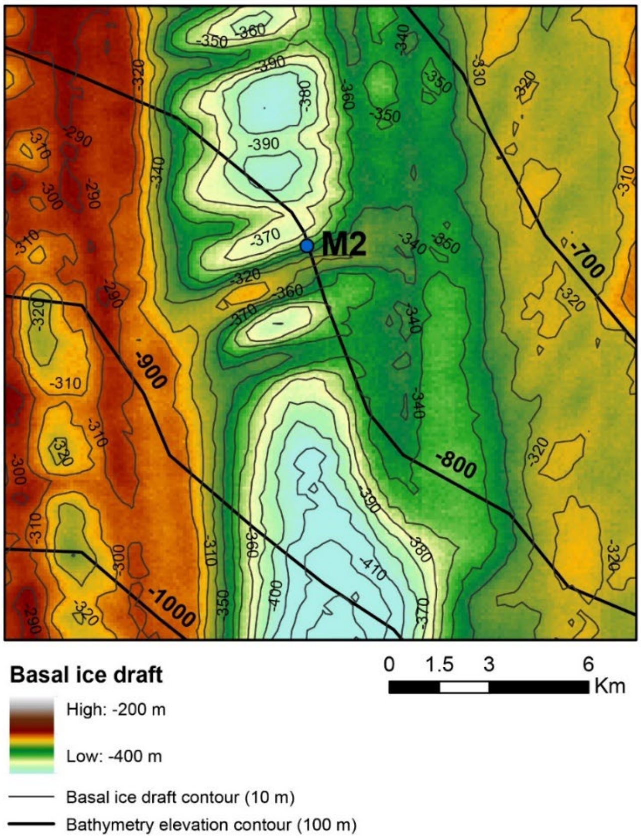

Figure S1. Basal ice draft and contour lines from a 2014 mosaic derived from the Reference Elevation Model of Antarctica (Morris et al. in prep., Howat et al. 2019) and bathymetric elevation (thick black lines; Arndt et al., 2013). The M2 site is marked in the map, where the ApRES and mooring is located.

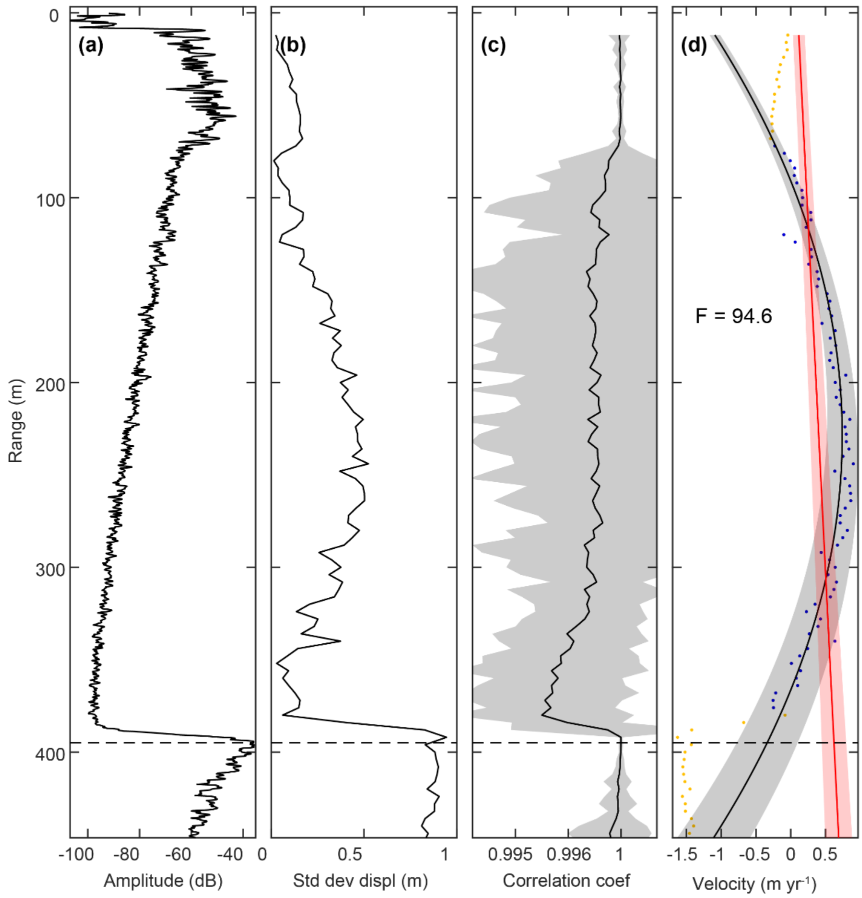

Figure S2. ApRES profiles with vertical strain rate estimation: (a) Return amplitude profile from a chirp averaged over the two-year-long record. (b) Standard deviation of the vertical displacement time series. (c) Mean cross-correlation coefficient with shading showing one standard deviation. (d) Mean velocity of internal reflectors. Blue dots mark velocities used to derive the vertical strain thinning at the base by fitting a linear (red) or quadratic (black) function. The F-test value is displayed for the preferred quadratic fit (Vaňková et al., 2021).

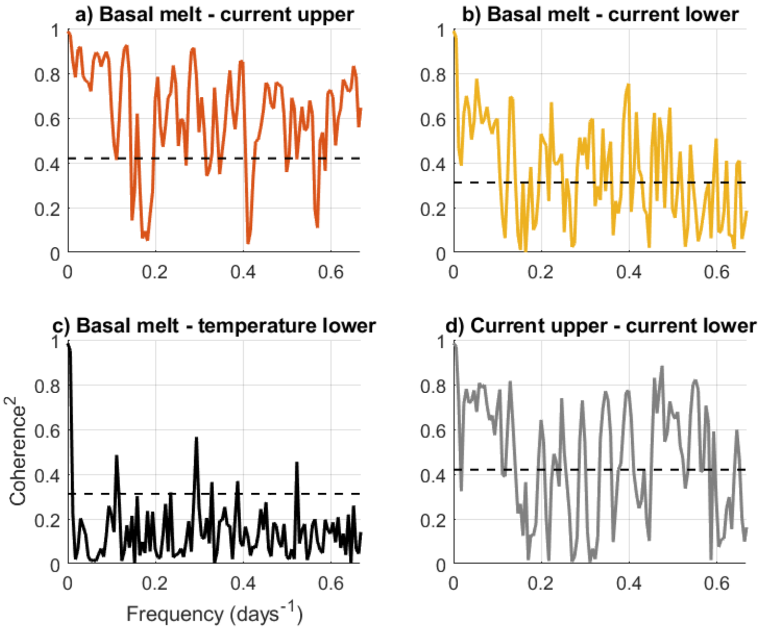

Figure S3. Magnitude squared coherence between 36-h filtered (a) basal melt and upper current sensor, (b) basal melt and lower current sensor, (c) basal melt and lower temperature sensor, and (d) upper and lower current sensor. The black dashed lines mark the 95 % confidence level.

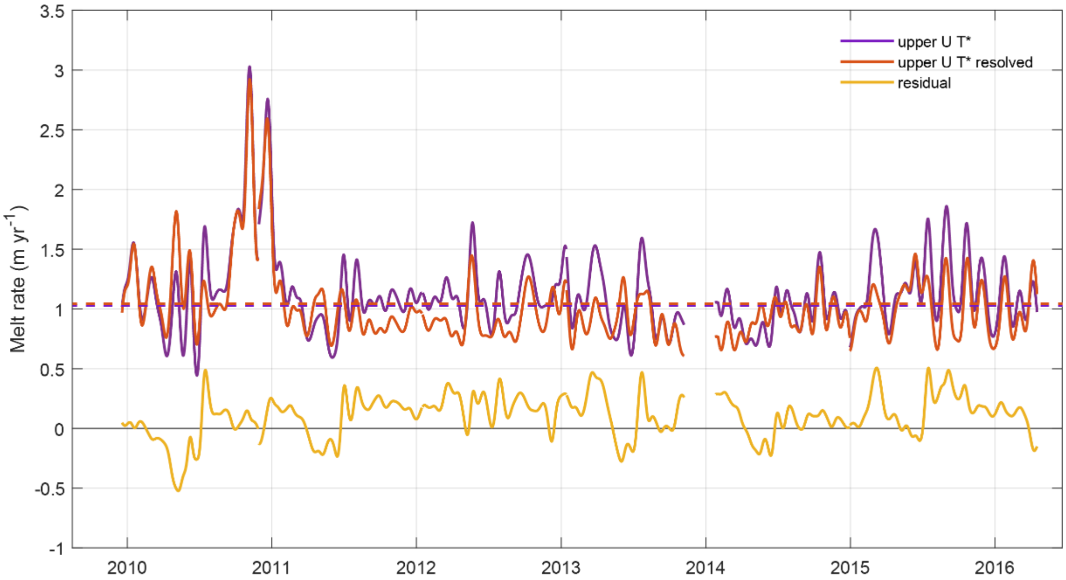

Figure S4. Influence of variable T* on parameterized melt for the pre-ApRES period. Mean values shown with a dashed line.

Symbol	Parameter	Value
c_i	Heat capacity of ice	2.0 x 10^3 J kg^{-1} $°C^{-1}$
c_w	Heat capacity of water	4.0 x 10^3 J kg^{-1} $°C^{-1}$
L_i	Latent heat of fusion of ice	3.4 x 10^5 J kg^{-1}
T_{*i}	Temperature in ice	–6 °C
$C_d^{1/2}\Gamma_{TS}$	Stanton number	4 x 10^{-4}
Γ_{TS}	The heat exchange coefficient	4 x 10^{-3}

Table S1. Physical constants used for melt parameterization and estimated effective thermal Stanton number.

References

Arndt, J. E., Schenke, H. W., Jakobsson, M., Nitsche, F. O., Buys, G., Goleby, B., et al. (2013). The International Bathymetric Chart of the Southern Ocean (IBCSO) Version 1.0 — A new bathymetric compilation covering circum-Antarctic waters. Geophysical Research Letters, 40, 3111–3117. https://doi.org/10.1002/grl.50413

Howat, I. M., Porter, C., Smith, B. E., Noh, M.-J., & Morin, P. (2019). The Reference Elevation Model of Antarctica, The Cryosphere, 13, 665–674, https://doi.org/10.5194/tc-13-665-2019.

Morris, A. (in prep.). Freeboard and thickness of Dronning Maud Land Ice Shelves from aligned strips of the Reference Elevation Model of Antarctica (REMA), (dataset doi to be provided for the final paper).

Taylor, J. R., (1996). An Introduction to Error Analysis: The Study of Uncertainties in Physical Measurements, University of Colorado.

Vaňková, I., Cook, S., Winberry, J. P., Nicholls, K. W., & Galton-Fenzi, B. K. (2021). Deriving Melt Rates at a Complex Ice Shelf Base Using In Situ Radar: Application to Totten Ice Shelf. Geophysical Research Letters, 48(7). https://doi.org/10.1029/2021GL092692